Dipole traps for neutral atoms formed by nonuniformly polarised Laguerre modes

A.V. Bezverbny, V.G. Niz'ev, A.M. Tymaikin

Abstract. **Field configurations of two counterpropagating nonuniformly polarised Laguerre modes forming three-dimensional dipole traps for neutral atoms are proposed. Peculiarities of the stochastic dynamics of atoms in such traps, associated with the anisotropy of dipole forces and manifestations of various radiative friction mechanisms are analysed. The problem of increasing the confinement time for atoms in such field configurations is studied.**

1. Introduction

Light beams with an annular intensity distribution $I(r)$ over the cross section (hollow-like beams) are used as optical dipole traps [1] for capturing atoms at the centre of the beam for field detunings $\delta > 0$ from the resonance frequency of the atomic dipole transition, when trapping is performed by the dipole force component directed along the radial gradient $I(r)$ (for $\delta < 0$, such a force causes a trapping of atoms in the transverse direction in a Gaussian light beam; this effect is used in nonresonance traps known as far-off resonance traps (FORT) [2]). Examples of such traps are the traps using resonator modes marked as TEM_{0l^*} [3] (l is the azimuthal number) with annular intensity distribution in the mode cross section (so-called doughnut modes).

Strictly speaking, doughnut modes are not modes in the accepted sense of the term. At a specific instant of time, a pure Laguerre-Gaussian mode TEM_{0l^*} (or a Hermite – Gaussian mode, which is transformed into the TEM_{0l^*} mode with the help of an astigmatic mode converter) is generated, but randomly turns around the axis, and hence the observed axially symmetric field distribution is the result of time-averaging [4]. Because of the random nature of such

A.V. Bezverbny Marine State University, Verkhneportovaya ul. 50a, 690059 Vladivostok, Russia; e-mail: alexb@mail.vntc.ru;
V.G. Niz'ev Institute of Laser and Information Technologies, Russian Acaemy of Sciences, Svyatoozerskaya ul. 1, 140700 Shatura, Moscow region, Russia; e-mail: niziev@laser.ru;
A.M.Tymaikin Institute of Laser Physics, Siberian Branch, Russian Academy of Sciences, prosp. Akad. Lavrent'eva 13/3, 630090 Novosibirsk, Russia, e-mail: tum@nsu.ru

a rotation, a strict axial symmetry of the $I(r)$ distribution cannot be guaranteed, and the resulting distribution in actual practice is intermediate between TEM_{0l^*} and the ideal axisymmetric distribution. Another peculiarity of such doughnut modes is their uniform polarisation, which is determined by the orientation of the polarisation-selective element in the cavity.

In this paper, we propose to use the nonuniformly polarised resonator modes (NPMs) as three-dimensional anisotropic traps for detunings $\delta < 0$, when the trapping is accompanied by a simultaneous cooling in all directions (down to sub-Doppler temperatures) of atoms with resonant dipole $J \rightarrow J + 1$ transitions. The peculiarities of the dynamics of atoms in such field configurations are studied.

2. Nonuniformly polarised Laguerre – Gaussian modes

It is well known that polarisation gradients are responsible for the emergence of additional forces whose action is of the same order of magnitude as the contribution of the intensity gradient, and which can qualitatively change the dynamics of an atom in the trap. It is also known that nonuniform polarisation can be attained in the cross section of a light beam by, for example, coherent extracavity superposition of two TEM_{01} modes with mutually orthogonal linear polarisations and mutually orthogonal mode axes [5]. This is accompanied by a simultaneous formation of an ideal axisymmetric distribution of the field amplitude. However, optical modes with an axisymmetric distribution of the polarisation (Fig. 1a) can be formed directly in the cavity if a polarised selective diffraction element is used as one of the mirrors [6]. Such nonuniformly polarised Laguerre – Gaussian modes (for the sake of simplicity, we shall consider the case $l = 1$ in the following analysis) are *the self-similar solutions of the vector wave equation* [7] for linearly polarised paraxial light beams in the form of a travelling wave. If the longitudinal component of the field is neglected, these solutions have the form

$$\boldsymbol{E} = \tilde{E}(r, z) \exp[\mathrm{i}\Phi(r, z)]\boldsymbol{e}_\alpha(\varphi),$$

$$\boldsymbol{e}_\alpha(\varphi) = \boldsymbol{e}_\alpha^*(\varphi) = \cos\alpha\,\boldsymbol{n}_r + \sin\alpha\,\boldsymbol{n}_\varphi, \tag{1}$$

where $\{\boldsymbol{n}_r, \boldsymbol{n}_\varphi, \boldsymbol{n}_z\}$ are unit vectors in the cylindrical coordinate system, and α is the angle between $\boldsymbol{n}_r$ and the local polarisation vector. Here the field amplitude has an annular distribution and the phase of field (1), unlike the TEM_{01} modes [8], does not contain an azimuthal dependence:

Figure 1. (a) Distribution of polarisation e in the NPM cross section, and (b) the distribution of polarisation e for a certain value of z in the case of superposition of counterpropagating NPMs.

$$\tilde{E}(r,z) = [N/w(z)]\rho \exp(-\rho^2),$$

$$\Phi(r,z) = 2\arctan\psi - \psi\rho^2 - 2\psi(z_0/w_0)^2, \tag{2}$$

where $\rho = r/w(z)$; $w^2(z) = w_0^2(1+\psi^2)$; $\psi = z/z_0$; $z_0 = \pi w_0^2/\lambda$; w_0 is the radius of the beam waist; and N is the normalising factor.

It is very important that the distribution of field E in NPMs is strictly axisymmetric at all instants of time. This enables us to form new field configurations in the case of extracavity coherent superposition of such waves. Consider the simplest version of two counterpropagating NPMs of identical intensity with polarisations e_{α_1} and e_{α_2} and the resultant field amplitude

$$\mathscr{E}(r,z) = (\boldsymbol{EE}^*)^{1/2} = \tilde{E}(r,z)$$

$$\times \{2[1 + \cos(2\Phi(r,z))\cos\theta]\}^{1/2}, \tag{3}$$

where $\theta = \alpha_1 - \alpha_2$ is the angle between the polarisations of counterpropagating waves. In the zeroth-order approximation in the diffraction parameter $b = (kw_0)^{-1} \ll 1$ (k is the wave number), the polarisation distribution

$$e(r) = \frac{\exp(\mathrm{i}\Phi(r,z))e_{\alpha_1} + \exp(-\mathrm{i}\Phi(r,z))e_{\alpha_2}}{\{2[1 + \cos(2\Phi(r,z))\cos\theta]\}^{1/2}} \tag{4}$$

is analogous to the lin-θ-lin configuration [9] formed by two counterpropagating linearly polarised plane waves with an angle θ between polarisations. The ellipticity parameter

$$\ell(r,z) = e(r)e(r) = \frac{\cos(2\Phi(r,z)) + \cos\theta}{1 + \cos(2\Phi(r,z))\cos\theta} \tag{5}$$

has a significant longitudinal gradient $\partial_z\ell \sim 1/\lambda$, while the gradient in the radial direction due to the curvature of wave surface modes is insignificant ($\partial_r\ell/\partial_z\ell \sim b^3$). This ratio can be increased ($\partial_r\ell/\partial_z\ell \sim b$) if, for example, at least one of the waves is first passed through a nonlinear crystal with the refractive index $n \sim I(r)$. Let us denote the refraction-induced phase delay $I_{\max}$ by β. For $\beta \leqslant \pi/2$, the spatial self-phase modulation of the beam can be neglected. In this case, the amplitude and polarisation of the configuration correspond to (3) and (4) with the substitution $\Phi(r,z) \to \Phi(r,z) \pm \beta G(r)$, where $G(r) = I(r)/I_{\max}$ is the transverse profile of the beam intensity.

In contrast to the one-dimensional lin-θ-lin configuration, we also have in this case a gradient of the angle of rotation ϕ of the major axis of the ellipse of polarisation in the plane $\{r, \varphi\}$ (Fig. 1b) with components [10]

$$(g_4)_j = \nabla_j\phi = \frac{\mathrm{Im}(e\nabla_j e^*)}{(1-\ell^2)^{1/2}} = \frac{(n_\varphi)_j}{r}, \tag{6}$$

where $j = 1, 2, 3$ are the Cartesian coordinate indices. Taking into account the general case $\beta \neq 0$, we will denote such configurations as NPM-θ-NPM in the following analysis.

3. Dynamics of atoms in NPMs

The nature of the dynamics of atoms in the NPM-θ–NPM configuration is determined by the interaction time t_{int}. For $t_{\mathrm{int}} \gg \gamma^{-1}$ (γ is the rate of radiative decay of the excited state), the interaction of an atom with the field is incoherent due to the contribution from spontaneous emission. For an ensemble of atoms, this regime corresponds to the kinetic stage of evolution over the translational degrees of freedom, while the dynamics of an individual atom is of stochastic type due to fluctuations of the dipole force during spontaneous and induced emission of atoms. In the semiclassical approximation for slow atoms ($kv \ll \gamma$), the vector and tensor structures of the dipole force $\langle\hat{\boldsymbol{F}}\rangle = \boldsymbol{F} = \boldsymbol{F}_0(r) + \hat{\mathscr{X}}(r)\boldsymbol{v}$ and the structure of the diffusion tensor in the momentum space $\hat{\mathscr{D}}(r) = \hat{\mathscr{D}}^{(\mathrm{sp})} + \hat{\mathscr{D}}^{(\mathrm{ind})}$, determining the intensity of fluctuations of the force operator $\hat{\boldsymbol{F}}$, are presented in Ref. [10] for arbitrary configurations of the monochromatic field. In the case of the NPM-θ-NPM configuration, their structures are:

$$\boldsymbol{F}_0 = \sum_{i=1}^{4} F_i\boldsymbol{g}_i, \qquad \hat{\mathscr{X}} = \hbar\sum_{l,n=1}^{4} X_{ln}\,\boldsymbol{g}_l \otimes \boldsymbol{g}_n,$$

$$\hat{\mathscr{D}}^{(\mathrm{ind})} = \hbar^2\gamma S \sum_{l,n=1}^{4} D_{ln}\,\boldsymbol{g}_l \otimes \boldsymbol{g}_n, \tag{7}$$

where, in accordance with Ref. [10], $\boldsymbol{g}_1 = \nabla\ln\mathscr{E}$ is the relative gradient of the field amplitude; $\boldsymbol{g}_3 = -(\nabla\ell)/[2(1-\ell^2)^{1/2}]$ is the ellipticity gradient; $\boldsymbol{g}_l \otimes \boldsymbol{g}_n$ is the direct product of the vectors; $S = |\Omega|^2/(\gamma^2/4 + \delta^2)$ is the saturation parameter of the dipole transition defined in terms of the Rabi frequency $\Omega(r)$ and the detuning δ; and the total phase gradient of the field is equal to zero ($\boldsymbol{g}_2 = 0$). The contribution $\hat{\mathscr{D}}^{(\mathrm{ind})}$ is due to induced transitions, while the structure of the contribution $\hat{\mathscr{D}}^{(\mathrm{sp})}$ from spontaneous transitions is defined in terms of the polarisation vector e and its complex conjugate vector e^*. The explicit form of the tensor $\hat{\mathscr{D}}^{(\mathrm{sp})}$ and coefficients F_l, X_{ln}, D_{ln} for the $J \to J+1$ ($J = 0, 1/2, 1$) transitions are given in Ref. [10].

The dynamics of a solitary atom is described by the Langevin equation in the dimensionless form:

$$\frac{\mathrm{d}\boldsymbol{P}}{\mathrm{d}\tau} = \boldsymbol{f}_0 + \mu\hat{\mathscr{X}}\boldsymbol{P} + \boldsymbol{f}, \quad \langle\boldsymbol{f}(0)\otimes\boldsymbol{f}(\tau)\rangle = \mu\hat{\mathfrak{D}}\,\delta(\tau), \tag{8}$$

where $\langle\boldsymbol{f}(0)\otimes\boldsymbol{f}(\tau)\rangle$ is the random force correlator; $\mu = (2\omega_{\mathrm{r}} \times t_{\mathrm{op}})^{1/2}$ is a small semiclassical parameter; $\hbar\omega_{\mathrm{r}} = (\hbar k)^2/(2m)$ is the recoil energy during emission of a photon; m is the mass of an atom; and $t_{\mathrm{op}} = (\gamma S)^{-1}$ is the optical pump time for the ground state of an atom upon saturation

$S < 1$. The characteristic time scale is $t_0 = t_{op}/\mu$ ($t = t_0\tau$); the characteristic scales for transverse ($R = r_\perp/w_0$) and longitudinal ($Z = kz$) sizes are different and their ratio is $b = (kw_0)^{-1}$; the momentum scale $p_0 = \hbar k/\mu$ ($p = p_0 P$). The dimensionless quantities f_0, $\hat{\mathfrak{x}}$, and $\hat{\mathfrak{D}}$ correspond to F_0, $\hat{\mathscr{X}}$, and $\hat{\mathscr{D}}$, respectively. Components of the vector f_0 and tensor $\hat{\mathfrak{x}}$ along each of the transverse indices r, φ have the order of smallness b compared to the longitudinal index z, so that $(f_0)_r \sim (f_0)_\varphi \sim b(f_0)_z$ and $(\hat{\mathfrak{x}})_{r,r} \sim (\hat{\mathfrak{x}})_{\varphi,r} \sim b(\hat{\mathfrak{x}})_{r,z} \sim b(\hat{\mathfrak{x}})_{\varphi,z} \sim b^2(\hat{\mathfrak{x}})_{z,z}$. However, all the components of the diffusion tensor $\hat{\mathfrak{D}}$ have the same order of magnitude as $(f_0)_z$ and $(\hat{\mathfrak{x}})_{z,z}$, since the contribution $\hat{\mathscr{D}}^{(sp)}$ from spontaneous transitions is determined not through the field gradients.

Apart from a strong anisotropy, the kinetics of an atomic ensemble in the NPM-θ-NPM configuration has the following salient features. Trapping of atoms by the force f_0 ccurs in the presence of the intensity gradient g_1 or the ellipticity gradient g_3, and the localisation centres for the $J \to J + 1$ transitions for a field detuning $\delta < 0$ will be determined by the intensity peaks and the circular polarisation regions ($\ell = 0$) [11]. The light pressure force $F_{0,\varphi} = F_4 g_4$ is proportional to the degree of circular polarisation ($F_4 \sim \mathscr{A} = (1 - \ell^2)^{1/2}$) and is qualitatively of a different (vortex) type, because it is directed along n_φ and prevents the trapping of atoms. The regular force component $\mu\hat{\mathfrak{x}}^s P$, where $\hat{\mathfrak{x}}^s$ is the symmetric part of the tensor, determines the radiative friction, and its contribution at the optimal choice of parameters must favour the formation of stable localised states in the atomic ensemble (similarly to the formation of dissipative optical gratings [12]). However, a prolonged localisation of atoms in the NPM-θ-NPM configuration seems to be unlikely because of the smallness of this contribution over the transverse degrees of freedom. Note that the transverse momentum generated under the action of a random force f can simply remove an atom from the effective region of action of the light field, while the longitudinal momentum causes a hopping of the atom between the centres of localisation.

4. Results of numerical simulation

Numerical simulation of the stochastic dynamics of a single atom by a step-by-step integration of the Langevin equation (8) has indeed revealed that the confinement times of an atom in the field configuration are insignificant for $\theta = 0$ and $\theta = \pi/2$.

Consider the $0 \to 1$ transition and the NPM-θ-NPM configuration under the condition $\beta = 0$, when there is no phase delay due to refraction in a nonlinear crystal. In this case, the nonzero values of the coefficients in (7) have the form:

$$F_1 = -\frac{2\hbar\delta S}{1 + 2S}, \quad \tilde{\delta} = \frac{\delta}{\gamma}, \quad v = \frac{i}{2} + \tilde{\delta}, \tag{9}$$

$$X_{11} = \frac{2\tilde{\delta}S(1 - 2S - 8|v|^2 S^2)}{|v|^2(1 + 2S)^3}, \tag{10}$$

$$X_{44} = \frac{2\tilde{\delta}S}{|v|^2(|v|^2 S^2 + 1 + S)(1 + 2S)},$$

$$D_{11} = \frac{S[|v|^2(1 + 12S^2 + 32|v|^2 S^3) + 2(1 - |v|^2)S]}{2|v|^2(1 + 2S)^3}, \tag{11}$$

$$D_{44} = \frac{S}{2(1 + 2S)}.$$

Thus, cooling in the azimuthal direction ($X_{44} < 0$) occurs for arbitrary values of S when $\tilde{\delta} < 0$, while X_{11} reverses its sign for $S_0 = [(3 + 8 \times \tilde{\delta}^2)^{1/2} - 1]/(8\tilde{\delta}^2 + 2)$. The sign reversal is explained by the fact that the Doppler mechanism, in which cooling occurs for detuning $\tilde{\delta} < 0$, dominates for $S \ll 1$, while the Sisyphean effect*, leading to a cooling for this transition for $\tilde{\delta} > 0$, plays a dominant role for $S > S_0$ [14]. Therefore, irrespective of the sign of detuning for $S > S_0$, radiative cooling and heating coexist in the directions g_1 and n_φ. However, the numerical experiment reveals that spontaneous emission is the main destructive factor in this case: the magnitude of the random force f remains quite high owing to the contribution $\hat{\mathscr{D}}^{(sp)}$ irrespective of the choice of the parameters $\tilde{\delta}$ и S, and hence atoms are ejected in the transverse direction in the course of propagation of the light beam. For example, for the optimal choice of the parameters $S(w_0) = 3$, $\tilde{\delta} = -6.5$, the localisation time t_{loc} of the atoms in the field does not exceed $\sim 10^3 t_0$.

For low levels of saturation of the $J > 0$ transitions in the NPM-$\perp$-NPM configuration of the field, the cooling mechanisms associated with the degeneracy of the ground state of the atom play the main role [15]. New aspects emerge in the anisotropy of the kinetic processes: although X_{11} remains proportional to S in this limit, the structure of the tensor $\hat{\mathfrak{x}}$ acquires terms that are independent of S and account for the sub-Doppler cooling. For example, the Sisyphean mechanism of cooling, equivalent to that described in Ref. [15] for the lin-$\perp$-lin configuration and associated with the ellipticity gradient g_3, is observed in the longitudinal direction z for $\delta < 0$, and is manifested in the radial direction also when $\beta \neq \theta$. Cooling in the azimuthal direction is due to the component with X_{44}. Irrespective of S, the contribution from X_{44} leading to sub-Doppler cooling for $\delta < 0$ is manifested in transitions with $J \geqslant 1$, and the cooling mechanism is equivalent to that presented in Ref. [15] for the $\sigma^+ - \sigma^-$ configuration and the $1 \to 2$ transition. However, the numerical experiment shows that the light pressure force $F_{0,\varphi}$, which is the highest in regions of a circularly polarised field, eventually draws the atom from the interaction region even if the random force is neglected.

For other angles θ in the NPM-θ-NPM configurations, numerical experiments showed that the stability of localised trajectories of an atom increased with decreasing θ (small angles $\theta \sim 0.1$ are optimal) and is extremely sensitive to the choice of parameters b, δ and μ. The parameter b characterises the diffraction-limited divergence of a Gaussian light beam and is small ($b \sim 10^{-2}$). Localisation of atoms in the radial direction is enhanced considerably with decreasing the waist radius w_0 due to an increase in the transverse

---

*This effect is absent in the direction of n_φ because it is caused by gradients of energy shifts $\hbar\Omega_i$ (which are independent of φ) due to the dynamic Stark effect. Here, the real quantities $\hbar\Omega_i$ depend only on $\mathscr{E}$ and ℓ, and are eigenvalues of the atomic states $|i\rangle$ diagonalising the operator $\hat{V}$ of dipole interaction between an atom and the field in the rotating wave approximation [13]: $\hat{V}|i\rangle = \hbar\Omega_i|i\rangle$. Accordingly, Ω_i is the Rabi frequency for these states.

components of the gradients g_1 and g_3 (for $\beta \neq 0$ in the latter case), but it is quite difficult to increase the value of β to ~ 0.1 by focusing the beams (this is due to the requirement of matching of longitudinal axes of such counterpropagating NPMs). Moreover, the effect of the longitudinal component $E(r)$ becomes significant in this case. The potential component F_0 of the force depends linearly on δ for a fixed saturation, and hence the holding of atoms is insignificant at small detunings ($|\tilde{\delta}| \sim 1$). For large values of $|\tilde{\delta}|$, the contribution of the dipole force fluctuations caused by induced emission becomes significant. The optimal order of magnitude of the quantity $\tilde{\delta}$ is ~ -10.

The parameter μ is the most critical parameter for the efficiency of dipole traps for the NPM-θ-NPM configuration. This parameter can be represented in the form $\mu = [T_{\rm rec}/(T_{\rm D}S)]^{1/2}$, where $T_{\rm rec}$ is the temperature limit corresponding to the recoil energy during emission of a photon, and $T_{\rm D}$ is the Doppler cooling limit. For example, $T_{\rm rec} = 1.2$ μK and $T_{\rm D} = 240$ μK for Na atoms. Hence, taking the condition $S < 1$ into account (which is important for sub-Doppler cooling), the order of magnitude of the parameter μ is ~ 0.1. The numerical experiment showed that for $\mu = 0.01$, the atom is confined stably in spatially localised states for an arbitrary long time, and variations in the parameter β almost do not affect the localisation. However, localisation of atoms becomes unstable already for $\mu = 0.08$ even for a tightly focused NPM. As a result, an atom that is located in the vicinity of the highest intensity field at a distance $r \sim w_0$ from the longitudinal mode axis for some time, goes to a distance $r \gg w_0$ due to fluctuations of the dipole medium. Figure 2a shows the transverse distribution of the atomic trajectory over a period $2 \times 10^4 t_0 \sim 10^6 \gamma^{-1}$ for $b = 0.1$, $\tilde{\delta} = -10$, $\mu = 0.08$ and $\beta = 0$, where the atom irreversibly moves away from the region of interaction with the field.

Nevertheless, stabilised localised states of atoms were observed even for $\mu = 0.1$. In this case, the confinement time was rather long ($\sim 10^6 t_0$ and longer). The numerical experiment shows that this requires an optimisation of the detuning as a function of J and an increase in the transverse ellipticity gradient due to contribution with $\beta \sim 1$. Figure 2b shows the transverse distribution of the atomic trajectory with $J = 1$ over a time $10^5 t_0$ for $\tilde{\delta} = -20$, $\beta = 0.7$ and $b = 0.045$. As compared to Fig. 2a, the localisation time for the atom in the region $r \sim w_0$ is at least an order of magnitude longer for much less stringent requirements for focusing of field modes in the cross section, characterised by the parameter b.

5. Discussion of results

The proposed configuration of a dipole trap has a strong spatial anisotropy: the sub-Doppler cooling due to ellipticity gradient and the gradient dipole force lead to the efficient trapping and confinement of individual atoms in the longitudinal direction within the range $\Delta z \ll \lambda$, while the localisation of atoms in the transverse direction occurs at a distance $r \sim w_0$ from the longitudinal axis of the configuration.

The trap has two types of attraction regions. The first type corresponds to the intensity maxima with linear polarisation of the field, where $F_{0,\varphi} \approx 0$, while the second type corresponds to regions with circular polarisation of the field, in which the atoms are trapped and localised in the longitudinal direction of the gradient force component $F_{0,\ell} = F_3 g_3$. Here, for small angles $\theta \sim 0.1$ between the polarisations of the counterpropagating modes, the combined action of the vortex force $F_{0,\varphi}$ and radiative friction in the azimuthal direction (contribution to $\mathscr{X}$ with coefficient X_{44}) leads to *a stable cyclic motion* of the atoms in the transverse plane. In the numerical experiment (see Fig. 2b), for example, an atom that was initially localised in the maximum intensity (the confinement time in this region was about 5 % of the experiment duration) moves into the circular polarisation region and performs circular motion perturbed by a random force. Thus, a prolonged localisation of atoms in the NPM-θ-NPM configuration is quite possible and is caused by the *combined action* of highly anisotropic force processes of capture and radiative friction, as well as diffusive processes (for the atomic momenta).
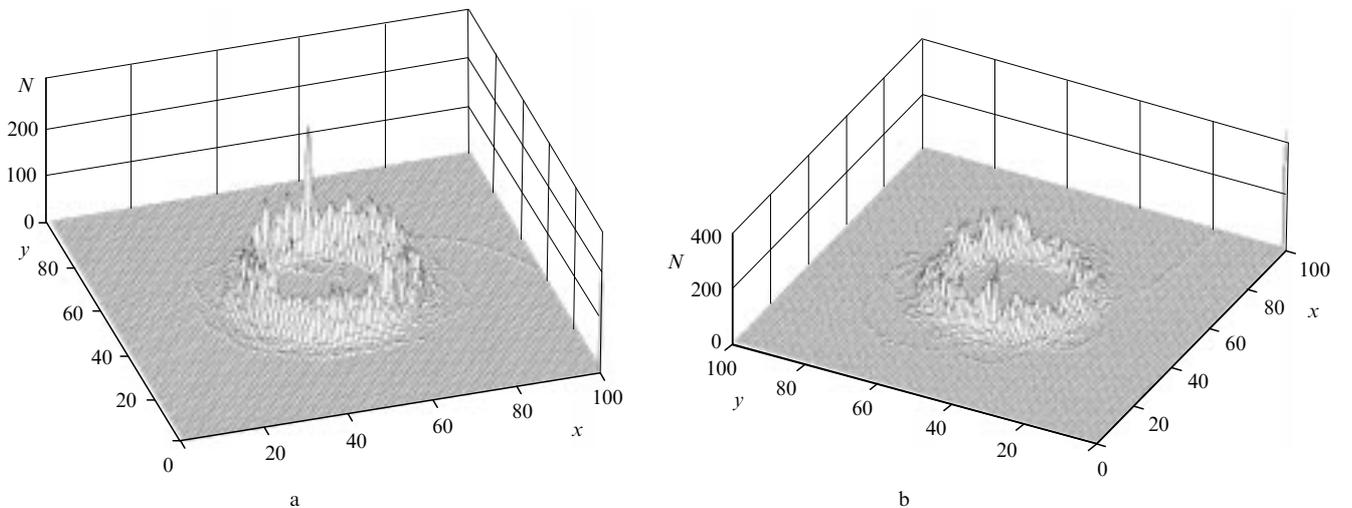
Figure 2. Distribution of the trajectory of an atom in the $\{r, \varphi\}$ plane for (a) $b = 0.1$, $\tilde{\delta} = -10$, $\mu = 0.08$, $\beta = 0$ and (b) $b = 0.045$, $\tilde{\delta} = -20$, $\mu = 0.1$, $\beta = 0.7$. The number N of attendances of cells is plotted along the ordinate, and the segment of the plane with boundaries $r \leqslant 2w_0$ is divided into 100×100 cells.

References

1. Grimm R., Weidemüller M., Ovchinnikov Yu.B, in *Advances in Atomic, Molecular and Optical Physics*. B. Bederson, H. Walther (Eds). (Cambridge: Acad. Press, 2000) pp 42–95.
2. Boiron D., Michaud A., Fournier J.M., Simard L., et al. *Phys. Rev. A,* **57**, R4106 (1998).
3. Kuga T., Torii Y., Shiokawa N., Hirano T. *Phys. Rev. Lett.,* **78**, 4713 (1997).
4. Solimeno S., Crosignani B., Di Porto P. *Guiding, Diffraction and Confinement of Optical Radiation* (Orlando, Acad. Press, 1986).
5. Kogelnik H., Li T. *Appl. Opt.,* **5**, 1550 (1966).
6. Nesterov A.V., Niziev V.G. *J. Opt. B,* **3**, 215 (2001).
7. Nesterov A.V., Niziev V.G. *J. Phys. D,* **33**, 1817 (2000).
8. Allen L., Beijersbergen M.W., Spreeuw R.J.C., Woerdman J.P. *Phys. Rev. A,* **45**, 8185 (1992).
9. Finkelstein V., Berman P., Guo J. *Phys. Rev. A,* **45**, 1829 (1992).
10. Bezverbny A.V., Prudnikov O.N., Taichenachev A.V., Tymaikin A.M., Yudin A.V. *Zh. Exp. Teor. Phys.,* **123**, 437 (2003).
11. Bezverbny A.V. *Laser Phys.,* **14**, 57 (2004).
12. Grynberg G., Robilliard C. *Phys. Rep.,* **355**, 335 (2001).
13. Visser P.M., Nienhuis G. *Phys. Rev. A,* **57**, 4581 (1998)
14. Dalibard J., Cohen-Tannoudji C. *J. Opt. Soc. Am. B,* **2**, 1707 (1985).
15. Dalibard J., Cohen-Tannoudji C. *J. Opt. Soc. Am. B,* **6**, 2023 (1989).